A Genome-wide CRISPR screen unveils WDR91 protein as a promoter of productive ASO activity

Grégory Menchon[1], Aris Gaci[2], Antti Matvere[1], Marc Aubry[1], Aurélien Bore[3], Aurélie Goyenvalle[2] and Rémy Pedeux[1*]

1 INSERM, OSS, UMR_S 1242, Univ. Rennes, 35000, Rennes, France
2 Université Paris-Saclay, UVSQ, Inserm, END-ICAP, 78000 Versailles, France
3 CRISPR'iT Genetic Platform Screening, Institut Curie, INSERM U934, CNRS UMR3215, 75005, Paris, France
*Corresponding author. Email: remy.pedeux@univ-rennes1.fr

ABSTRACT

Antisense oligonucleotides (ASOs) belong to promising therapeutic molecules for the treatment of neurologic, muscular and metabolic disorders. Ten ASOs have been approved so far and many of them are in advanced clinical development covering a dozen therapeutic areas including cancer. Yet, their mechanisms of internalization, cell trafficking and action of these molecules remain poorly understood. Moreover, with an estimated 1% of ASO reaching the correct cellular compartment following systemic delivery, the majority of targeted diseases requires recurrent injections of ASOs. A deeper understanding of these mechanisms would guide the improvement of their efficiency and thus, reduce the amount of delivered ASOs and their potential side-effects. Here, we performed a genome-wide CRISPR knockout screen and identified several proteins which could significantly impact ASO potency in a melanoma cell line. From these candidates, we validated WD Repeat Domain 91 (WDR91) as a modulator whose depletion strongly inhibits ASO activity in melanoma. WDR91 is known as a regulator of endosomal maturation, suggesting that ASOs productive release in cytosol could mainly occur during early endosome maturation or from the late endosomes as supported by other studies. We show that this effect is also observed in another cell line with a different assay, ASO chemistry and mode of action, which could highlight a general mechanism that positively impacts ASOs trafficking in cells.

INTRODUCTION

Synthetic Antisense Oligonucleotides (ASOs) belong to a class of attractive therapeutic compounds for numerous diseases. ASOs modulate cellular target gene expression through Watson-Crick binding to complementary RNA molecules and, according to their type, act by either promoting a RNAse-H1 mediated RNA degradation (Gapmers - GMs) or through a steric blocking mechanism (mixmers and target site blockers – TSBs) leading to three major modes of action: gene-expression inhibition or activation and splicing modulation[1]. ASOs have been used for treating different genetic disorders and they can be translated to personalized therapies[2]. ASOs are specially taken up by fast growing cells[3] and, among numerous advantages, bypass the current bottleneck regarding the targets that are considered undruggable with traditional small molecule inhibitors[4]. To date, ten ASOs are currently approved by the FDA for genetic and rare diseases[5,6] and several phase II and III studies are ongoing in the oncology therapeutic area[7].

Although ASOs promise a great leap forward in future cancer treatments, their utilization suffers from major hurdles. Among them, a lack of tissue specific targeting[8,9] , poor cellular

uptake[10] and the need to escape form the endo-lysosomal pathway to exert their role in either the cytoplasm or nucleus of the cells[11,12]. Moreover, the mechanisms of internalization, cell trafficking and action of these molecules remain poorly understood. An estimated 1% of ASO reaching the correct cellular compartment and target following systemic delivery[13,14] leads to treatments consisting of high doses, recurrent injections and thus, significant accumulation in other non-targeted cells and organs with consecutive toxicities[15]. It is therefore essential to better understand the fate of internalized ASOs and their intracellular route and mode of action. Such deeper characterization in different cell lines with different ASO types and chemistries would help in the rational design and improvement of therapeutic ASO strategies in future clinical applications. It has been demonstrated in many studies that the fate of internalized phosphorothioate (PS)-containing ASOs was determined by intracellular interacting proteins[16,17,18]. Even if a clear mechanism is still to be fully understood, around 80 intracellular proteins have been identified and this protein interactome appears to influence the pharmacological activities and potential toxicities of PS-ASOs by acting on their uptake and distribution. It is also worth noting that many other proteins that bind to ASOs have no effect on their activity. Considering that PS-ASOs are internalized and processed through the endocytic pathway[19,20], other proteins should be considered such as protein modulators that do not directly interact with the oligonucleotides but rather act on the endosomal trafficking and maturation until a fraction of the cargo escape from the endocytic organelles. Several studies have investigated the modulation of intracellular pathways to increase the productive delivery and activity of oligonucleotides and to further unveil the critical molecular factors that contribute to nucleic acids pharmacological effects[21]. Among these, modulation of endocytic recycling[22,23], multivesicular bodies' (MVBs) fusion with lysosomes[24], endosomal escape[25] and nuclear shuttling[26,27] were explored. All these strategies involve the use of either genetic or non-genetic perturbations and have proven to be successful in many *in vitro* and *in vivo* studies. ASO-interacting proteins have been mostly characterized by *in vitro* studies using pull-down experiments on cell lysates[28,29] but such method lacks physiological relevance as the intracellular membrane's integrity is not preserved and could lead to many binding artefacts. Furthermore, pull-down studies may highlight some important ASOs protein modulators but only allow the identification of direct interactants. To circumvent these issues other authors recently used proximity biotinylation assay to highlight oligonucleotides interactome in living cells and in pharmacologically relevant conditions[30].

Clustered Regularly Interspaced Short Palindromic Repeats (CRISPR) screen is a powerful genetic perturbation method that can be used for functional genomic studies, by activating or silencing genes[31]. Often used to characterize the genes that make a cell resistant or sensitive to a particular drug, it can also be implemented to identify ASOs direct and indirect modulators in a more physiological state and preserving the cell membrane's integrity. This technique was implemented in different studies to investigate modulators of dsRNAs[32], Antibody-Drug Conjugates (ADCs)[33] or encapsulated mRNAs[34], but to our knowledge, a single recent study describes such a functional genomic screen (CRISPR gene activation) to uncover factors enhancing ASOs activity[35]. In the present work, we used a genome-wide CRISPR screen strategy (CRISPR knockout), to uncover proteins that increase the potency of a tricyclo-DNA (tcDNA) based-ASO in a melanoma cell line (501Mel). The screen was performed without *a priori* on 19,114 coding genes with the Brunello CRISPR knockout library. Out of the sorted candidates, we unveiled and further validated WDR91 as a positive regulator of ASO activity.

RESULTS

Development and *in vitro* validation of a tcDNA-ASO to inhibit 501Mel cells proliferation with a target-site blocking mechanism

Previous work aiming at masking a microRNA target site on a microRNA sponge (TYRP1 mRNA) led to the test and validation of a commercially-designed Locked Nucleic Acid (LNA) TSB (named TSB-T3 for Target-Site Blocking – T3), that significantly induced the reduction of melanoma tumor growth *in vitro* and in 501Mel PDX mice[36]. TSB-T3 exerts its ASO activity by preventing the sequestration of the miR-16 tumor suppressor by TYRP1 mRNA and redirecting it towards its target-RNAs like RAB17, to induce their decay and subsequently reduce tumor proliferation (Figure 1A).
We first decided to design and evaluate a new TSB-T3 with the same sequence as the former commercial one but with a full tcDNA chemistry and phosphorothioate (PS) backbone. This class of conformationally constrained ASO displays enhanced binding properties to DNA and RNA as well as unique pharmacological properties and unprecedented uptake by many tissues after systemic administration[37,38].
501Mel cells were reverse-transfected in 96-well plates with both LNA- and tc-TSB-T3 at doses ranging from 10 to 70nM. After 72h, the cell density was measured by colorimetric assay and normalized to a control ASO treatment (tc-TSB-C1).
As expected, we observed a dose-response anti-proliferative activity with both chemistries but a higher potency with the tc-TSB-T3 (Figure 1B). A western blot analysis confirmed the decay of RAB17 protein in tc-TSB-T3 treated cells by comparison with the tc-TSB-C1 (Supp. Figure 1A). We thus chose to continue with the tc-TSB-T3 oligonucleotide in the next CRISPR screening experiment.

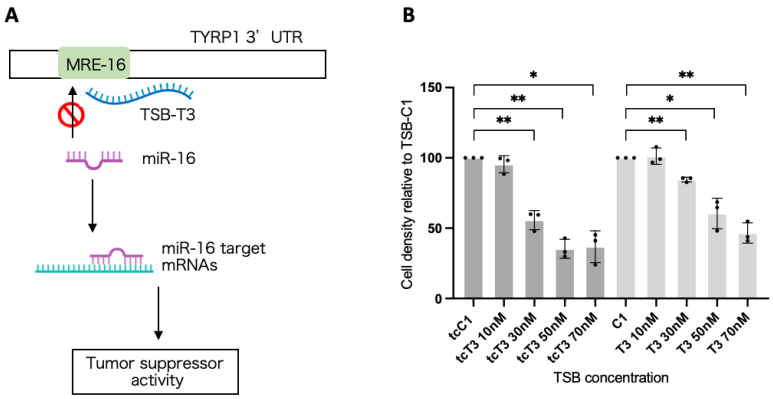

Figure 1. Inhibition of 501Mel cells proliferation with Target Site Blocker ASOs targeting TYRP1 mRNA. (A) A competition mechanism occurs with binding of TSB-T3 to a sequence overlapping the miR-16 site in the 3'UTR of TYRP1, thus releasing miR-16 whose tumor suppressor activity is restored. Gilot *et al*, 2017, modified. The figure 1A was generated with BioRender.com (B) 501Mel cell density assay at day 3 with increasing concentrations of reverse-transfected LNA- (T3) or tc-TSB-T3 (tcT3). Experiments were performed in biological triplicate. Error bars represent standard deviation.

Genome-wide pooled sgRNA library generation, knockout library treatment with tc-ASOs and NGS sequencing

The CRISPR-knockout cell library was generated by infecting 501Mel cells with a pooled lentiviral library which contains the Cas9 and sgRNAs targeting all the coding genes. This lentivirus library contained 4 different guides per coding gene (total of 76.442 sgRNAs). Infected cells were positively selected with antibiotic, expanded and subsequently transfected with either the tc-TSB-T3 or -C1 ASOs. At the end of each respective treatment, cells were pooled and a pellet of 100 million cells per condition was used for genomic DNA (gDNA) extraction and PCR amplification of the integrated sgRNAs in the 3 samples (initial non-treated cell library, tc-TSB-T3 treated and tc-TSB-C1 treated). Amplicons were purified and a verification on a TapeStation system confirmed the quality of the final samples regarding the expected size, purity and concentration (Supp. Figure 2). The global pipeline is depicted in Figure 2A.
After amplicons sequencing by the NGS platform, a quality check was performed and we observed only 115 not detected sgRNAs over 76.442 in our cell library, which validated proper conditions before ASOs treatment. The normalized reads count in each initial library, control and therapeutic ASO condition were plotted and provided a mean of 400-500 reads per guide as expected (Figure 2B).

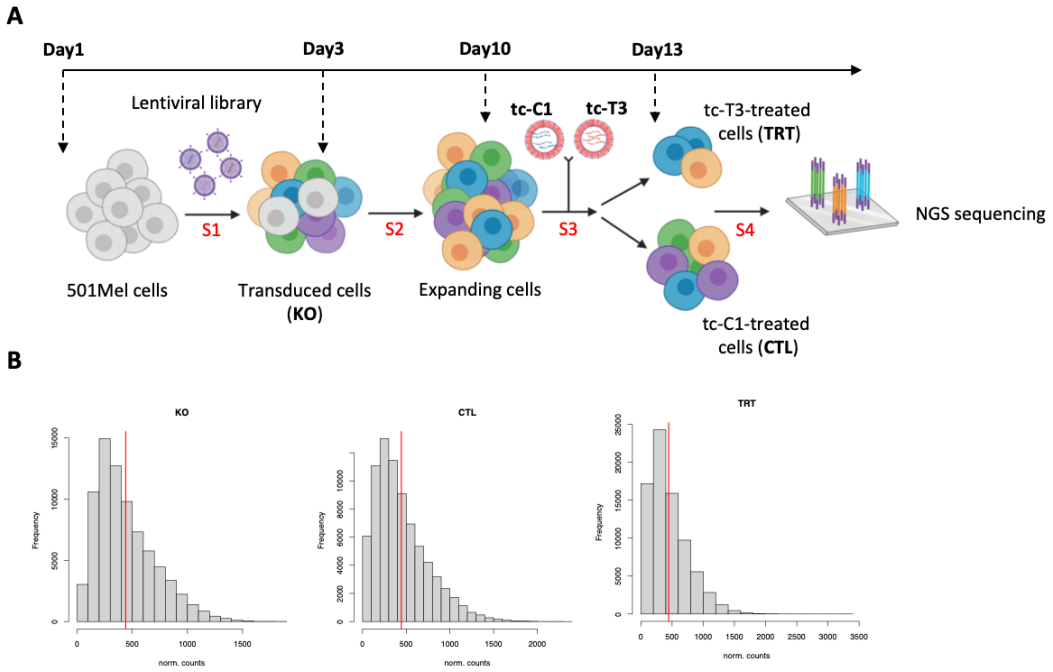

Figure 2. Generation and treatment of the 501Mel cells knockout library. (A) Pipeline of the experimental setup. S1: Step 1 (cells transduction); S2: Step 2 (transduced cells positive selection); S3: Step 3 (ASO reverse-transfection); S4: Step 4 (gDNA purification and sgRNAs amplification). (B) Distribution of the number of normalized read counts per sgRNA in the initial transduced library (KO), the tc-TSB-T3 treated library (TRT) and the tc-TSB-C1 treated library (CTL). The mean is represented by a red bar. The figure 2A was generated with BioRender.com.

Sequencing data analysis and identification of proteins promoting tc-TSB-T3 productive activity in 501Mel cells

To identify proteins that could positively impact the tc-TSB-T3 activity in 501Mel cell line, the NGS sequencing raw data accounting for the total number of sgRNA reads per gene and per

sample were analyzed as follows. First, MAGeCK extraction, normalization and sorting was performed for the sgRNA read counts from the C1- and T3-treated cells. Then, MA Plots were obtained and top candidates extracted after using the following cutoff for the 4 sgRNAs per gene: A (mean average) ≥ 6 and M (log ratio) ≥ 0.6 (fold change T3 *vs* C1 ≥ 1.5) (Figure 3A). In 501Mel cells, a treatment with tc-TSB-T3 significantly impedes the cells growth since the tumor suppressor miR-16 is released from TYRP1 mRNA. We hypothesized that the cells containing a sgRNA inducing the depletion of a protein involved in ASO uptake and/or efficiency will better survive and be enriched after treatment with the therapeutic tc-TSB-T3 ASO by comparison with the control tc-TSB-C1 ASO. Thus, by comparing the sgRNAs enrichment in treated *versus* control conditions, we sought to identify proteins potentially involved in ASO productive uptake, trafficking, release and guidance to their RNA-target. As shown in Figures 3B-C, the selected cutoff allowed to highlight a first set of 5 genes with the 4 sgRNAs fulfilling the chosen criteria (ELMOD1, FH, SMOX, TADA2B and WBSCR16). Apart from SMOX (which had the smallest fold changes), these genes were selected and considered as a nonbiased sampling of potential candidates. It is worth noting that from this list, WBSCR16 (Williams-Beuren Syndrome Chromosomal Region 16) appeared as the strongest candidate based on the fold change of the 4 individual sgRNAs.

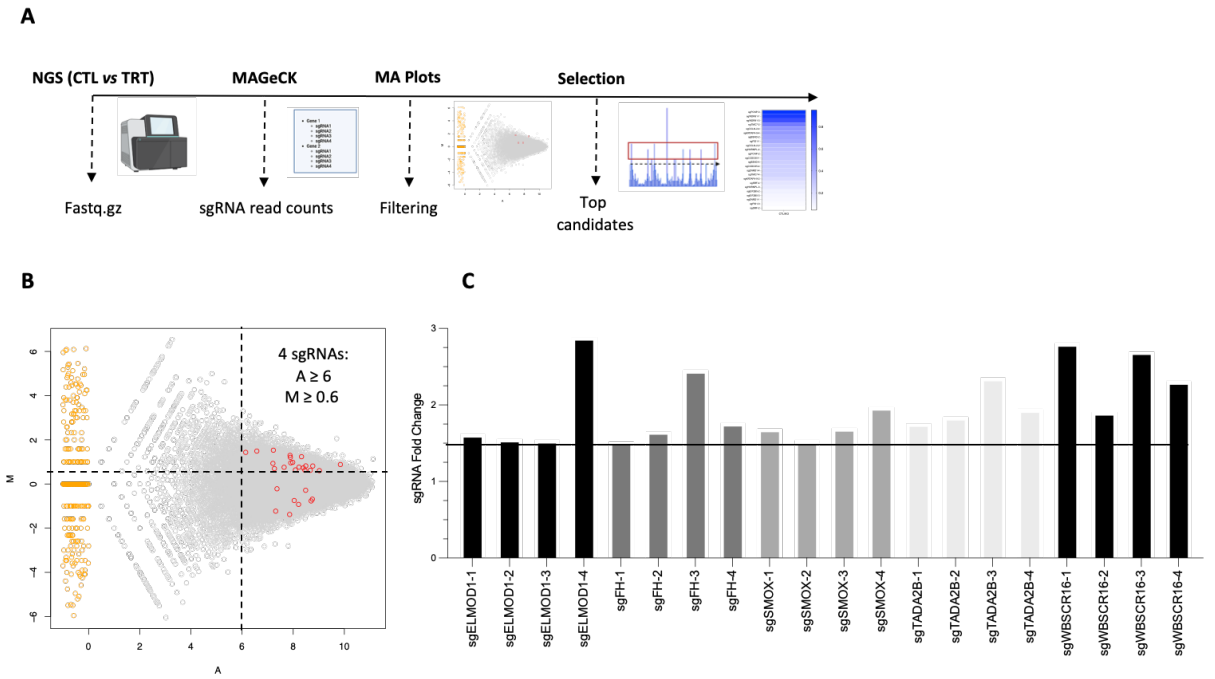

Figure 3. NGS sequencing data sorting and primary candidates' selection. (A) After sgRNA extraction, MA plots are used to visualize the differences between measurements (read counts) between two conditions: TRT (tc-T3) *versus* CTL (tc-C1). For each sgRNA, the read counts are transformed onto M (log ratio) and A (mean average) scales. M is equal to log2(sgRNA_count_in_TRT+1) - log2(sgRNA_count_in_CTL+1) and A is the mean between count_TRT and count_CTL in log2 scale. Candidates selection was performed according to the following criteria: A ≥ 6 and M ≥ 0.6. (B) MA plot from the selected candidates with applied M and A filters. (C) Fold-changes between TRT and CTL conditions of each 4 sgRNA from the top 5 candidates. The figure 3A was generated with BioRender.com.

By sorting the candidates considering 3 guides out of 4 with the criteria A ≥ 6 and M ≥ 0.6 (fold change T3 *vs* C1 ≥ 1.5), we obtained a list of 31 supplementary gene candidates (Supp. Figure 3A and B).

We also considered the genes with at least 2 guides out of 4 fulfilling the following criteria: A ≥ 6 and M ≥ 1 (fold change T3 *vs* C1 ≥ 2). As shown in Figures 4A and B, this new cutoff allowed to highlight a set of 66 genes with at least 2 sgRNAs fulfilling the chosen criteria. For a more stringent selection of candidates, we decided to focus only on the genes with the highest fold changes and reduced the list to the following 12 genes: BSND2, WDR91, CCDC65, CDC42, EIF2B5, FIS1, HNRNPL, KRTAP4-9, PCNP, SRF, TMC7 and ZNRD1 (Figure 4B, light and dark blue bars). Then, we discarded the genes with a significant difference between the number of reads in the initial non-treated library and the tc-TSB-C1 treated cells (low C1 reads number / Library reads number ratio). From this last step, only WDR91 gene had both sgRNAs with a high 0.8 and 0.9 ratio (Figure 4B and C, dark blue bars).
Finally, we chose to keep only the candidates obtained with the most stringent filters. Of the 102 initial proteins, we selected WDR91, ELMOD1, FH, TADA2B and WBSCR16 for further functional validation.

A similar analysis was performed by looking at the sgRNAs depletion in treated *versus* control conditions, to identify proteins that negatively impact ASO activity (Supp. Figure 4A and B). Indeed, cells containing a sgRNA inducing the depletion of a protein that negatively regulates ASO release and potency will survive less and end up depleted after treatment (ASO more efficient). By sorting the inhibitor candidates considering 2 to 4 sgRNAs with the criteria A ≥ 6 and M ≤ -1, we obtained a list of 52 candidates.
However, we decided to focus on protein activators of ASOs for subsequent validation experiments since extracting information from enriched cells population is more reliable from a technical aspect.

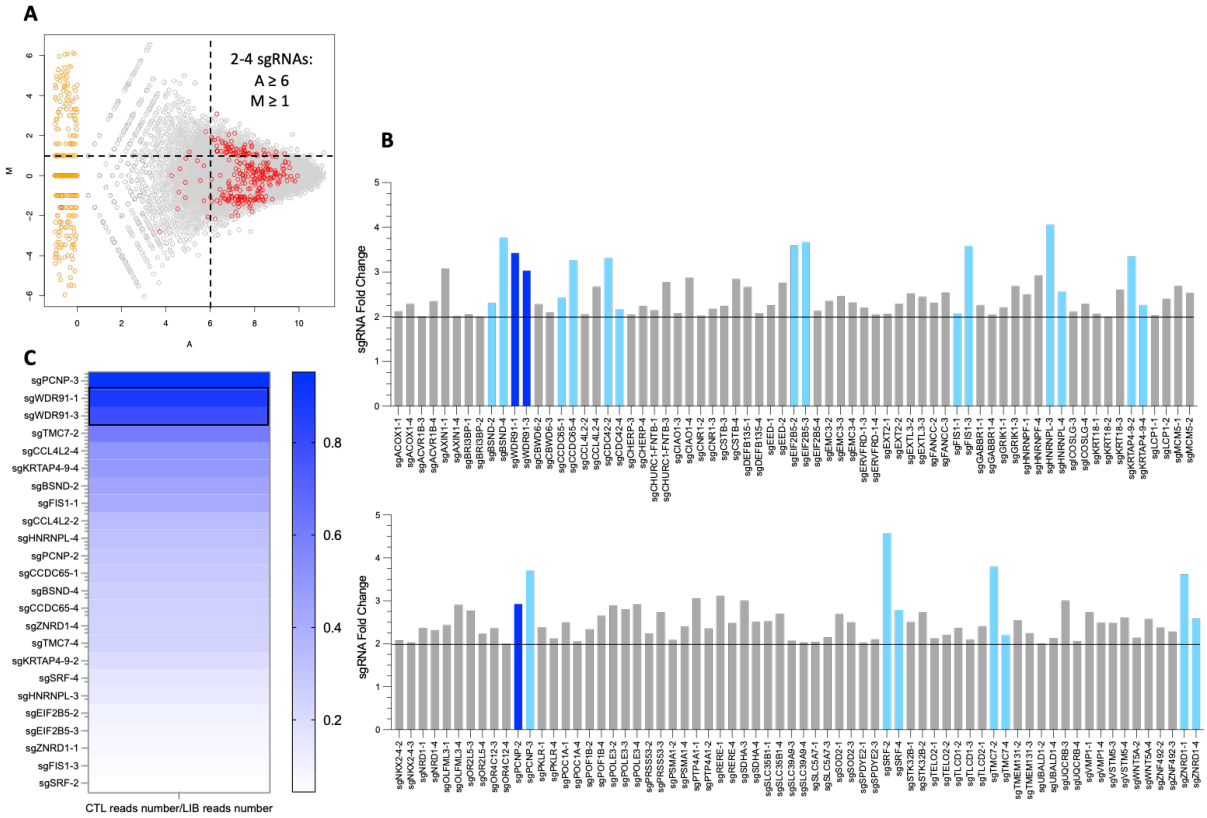

Figure 4. Secondary candidates' selection. (A) MA plot from the selected candidates with applied M and A filters. (B) Fold-changes between TRT and CTL conditions of each 2 to 4 sgRNA from the top 66 candidates (with at least 2 guides over 4 with a fold change ≥ 2). Light blue bars represent the 12 selected

candidates with the highest fold changes. Dark blue bars represent the candidates with the higher C1 reads number / Library reads number ratio (WDR91 and PCNP). (C) Heat map representing the C1 reads number / library reads number for the 12 selected candidates with the highest fold changes.

Validation of the tc-TSB-T3 activity enhancer candidates by RNA interference and 501Mel cells proliferation assays

An RNA interference experiment was designed to further validate our five candidates as ASO activity enhancers. After protein knockdown, the tc-TSB-T3 activity should be reduced resulting in increased cell proliferation compared to a control condition. The global experimental pipeline is depicted in Figure 5A.

It was already well established in former *in vitro* studies that the protein Annexin A2 (ANXA2) was an important facilitator of PS-ASOs endosomal trafficking in different cell lines[39]. We thus first evaluated the effect of ANXA2 downregulation in 501Mel cells proliferation with or without tc-TSB-T3 in comparison with a control siRNA. A western blot analysis confirmed the decay of ANXA2 protein after cells treatment with an ANXA2 siRNA (Supp. Figure 1B). As shown in Figure 5B, ANXA2 knockdown significantly impaired the activity of tc-TSB-T3 by comparison with a control siRNA. We thus decided to include this protein as an enhancer positive control in our assays.

Each individual candidate (WBSCR16, TADA2B, FH, ELMOD1 and WDR91) was downregulated with a corresponding siRNA (or a control siRNA) for 48h. 501Mel cells were then reverse-transfected with either the siRNA alone or a combination of siRNA and tc-TSB-T3. Four days after the second transfection, the cell viability was measured by a crystal violet colorimetric assay.

After normalizing the cell density in each condition with the non-treated one, both WBSCR16 and WDR91 knockdown cells showed a significant and reproducible inhibition of tc-TSB-T3 anti-proliferative activity, with WDR91 having the strongest effect (Figure 5B). Therefore, we decided to focus our investigation on WDR91.

Melanoma cells proliferation can also be promoted by the level of TYRP1 mRNA expression[40]. Thus, to discard any biased effect on the observed proliferation rate induced by TYRP1 mRNA level changes upon siRNA transfection, we performed qPCR analysis on siRNA reverse-transfected cells. Our results show that TYRP1 mRNA expression level is not significantly affected by the transfection of control, ANXA2 or WDR91 siRNAs (Supp. Figure 5).

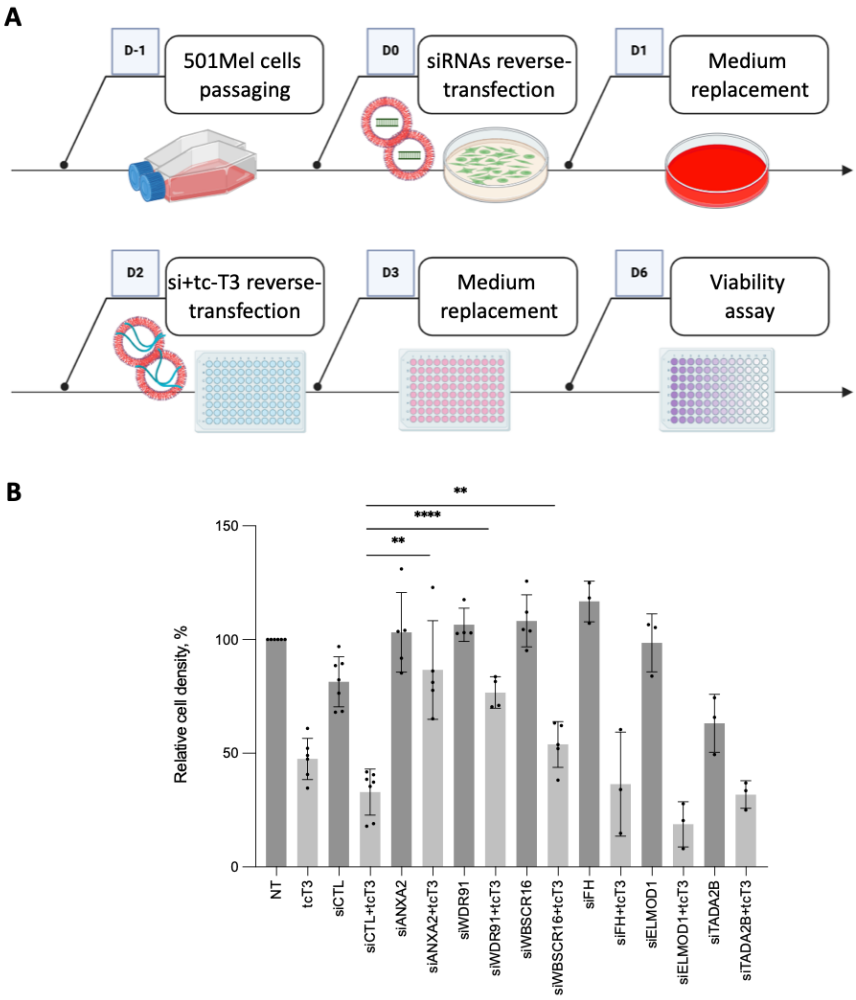

Figure 5. Functional validation of tc-TSB-T3 activity enhancer candidates in 501Mel cells. (A) Pipeline of the experimental setup. (B) 501Mel cells proliferation assay after tc-TSB-T3 transfection on normal, control or candidate's knock-down cells (NT: Non-Treated; CTL: control siRNA). The relative cell density was normalized to the non-treated cells. Results are shown as the average of independent biological replicates ± SD. P-values were calculated by two-sided unpaired *t*-tests with Welch's correction. **** P <0,0001.

WDR91 participates in PS-ASO productive release and activity in different human cells independently of the ASO type and chemistry

We decided to investigate whether WDR91 could be a general positive regulator of PS-ASO trafficking and productive activity in different transfected cell lines. Indeed, our analysis was performed in 501Mel cells and it is known that human cancer cell lines have very heterogenous ASO uptake efficiencies[41]. Moreover, we identified WDR91 using a fully modified TSB ASO made of tcDNA and wondered whether similar effect would hold true in a different system (different mechanism of action, chemistry and cell line). To address this question, we decided to transfect the U2OS osteosarcoma cell line with siRNAs directed against WDR91 and evaluate the effect on an LNA Gapmer (GM) activity directed against Inhibitor of Growth Family Member 2 (ING2) mRNA. ING2 protein is part of a family of epigenetic regulators that are involved in DNA replication, DNA damage response and apoptosis[42]. Our assay's read out only focused on ING2 mRNA levels quantifications after WDR91 protein knockdown and GM transfection. WDR91 was downregulated by reverse-transfecting U2OS cells at low confluency with a corresponding siRNA for 48h followed by a second transfection with the ING2 GM.

Two days after the second transfection, total RNAs were extracted and ING2 mRNA level was determined by quantitative PCR. The global experimental pipeline is depicted in Figure 6A. When analyzing the ING2 mRNA level normalized to the non-treated condition, it appears significantly higher in the WDR91 knockdown cells compared to the control siRNA cells (Figure 6B). The ING2 GM productive activity is then impaired in WDR91 knockdown cells.

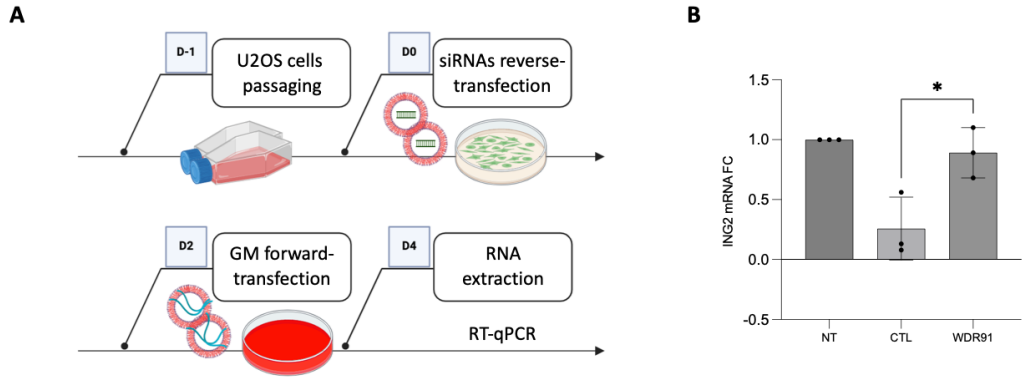

Figure 6. Functional validation of WDR91 in U2OS cells. (A) Pipeline of the experimental setup. (B) U2OS cells proliferation assay after ING2 Gapmer transfection on non-treated, control or WDR91 knock-down cells (NT: Non-Treated; CTL: control siRNA). The relative ING2 mRNA fold change was normalized to the non-treated condition (no siRNA transfection). Results are shown as the average of three independent biological replicates ± SD. P-value was calculated by two-sided unpaired *t*-tests with Welch's correction. * P <0,05.

Taken together, these results unveil WDR91 as an ASO positive regulator in two different cell lines. We postulated that this protein could be a general indirect modulator of ASOs productive release independently of the cell line and ASO type and chemistry.

DISCUSSION

Despite many clinical successes, clear mechanisms of ASOs uptake and trafficking remain to be fully understood. CRISPR genetic screen is a powerful strategy to highlight protein modulators that can act by either promoting or preventing ASOs activity in cells. In this study, we used a genome-wide CRISPR inhibition screen to identify without *a priori* proteins involved in productive tricyclo-ASO trafficking, release and activity in a 501Mel cell line. After cells transduction by a knockout lentiviral library and selection, a treatment with our specific ASO molecule (and a non-targeting control ASO) was performed for three days and the surviving cells were recovered for guide RNA enrichment sequencing. We hypothesized that at a relatively high ASO concentration, most of the cells within the CRISPR cell library should experience a significant proliferation inhibition except for the cells with a potential ASO-promoting protein being knocked-out. For this study, we used the 501Mel cell line as this model and the corresponding ASO (with LNA chemistry) were already used and validated in a former study investigating a non-coding function of TYRP1 mRNA promoting melanoma growth[43]. Only few information is available in the literature regarding the identification of intracellular protein modulators of ASOs by genetic perturbations. Our CRISPR knockout screen strategy strengthens this field and allows to uncover such candidates (with either an active or passive

role), with a 3rd generation ASO and preserving the integrity of intracellular membranes and organelles.

After sequencing, MA plots analysis with defined average expression and fold change parameters revealed a set of 102 and 54 potential ASO enhancers and inhibitors, respectively. However, to counteract the low power of this pilot study, we chose to apply rather stringent filters to identify robust ASO activity modulators and exclude false positives. Our screen highlighted both WBSCR16 and WDR91 proteins as candidates of interest. WBSCR16 protein is associated to the inner mitochondrial membrane and has been suggested to be an essential Guanine Nucleotide Exchange (GEF) factor involved in mitochondrial fusion[44]. Considering that mitochondria can physically and functionally interact with endosomes[45,46], we cannot exclude the possibility that the ASO is internalized into the mitochondria and is further released in the cytosol during the fusion process. Further validation experiments would be required to investigate the impact of WBSCR16 on other types of ASO potency.

By looking at the supplementary candidates (considering 3 guides out of 4 with the criteria A ≥ 6 and M ≥ 0.6 (fold change T3 *vs* C1 ≥ 1.5), two of them (Xylosyltransferase 2 - XYLT2 and Conserved Oligomeric Golgi complex 8 - COG8) attracted our attention. XYLT2 is an enzyme which is involved in the biosynthesis of glycosaminoglycan chains in proteoglycans, including heparan sulfate[47]. COG8 is a component of the COG complex which is involved in intra-Golgi membrane trafficking[48]. These two proteins might be included in the set of indirect positive ASO regulators. Indeed, Olivier Petitjean *et al*, revealed in 2020 an important role of the heparan sulfate pathway and the conserved oligomeric Golgi complex in the double-stranded RNA uptake and transfection efficiency[49]. During the same year, Xue-Hai Liang *et al*, published a study regarding the facilitation of ASOs release from endosomes by the Golgi-endosome transport[50]. It would be then meaningful to introduce the full panel of COG proteins in future investigations for ASOs modulators. However, and regarding the known contribution of heparan sulfate decorations in the cell docking of lipoplexes[51,52], the related proteins involved in the heparan sulfate biosynthesis might not be critical in the case of naked oligonucleotides (delivery without any cationic lipids carrier).

We confirmed WDR91 as a positive modulator of ASO activity in two different assays, cell lines and ASO types and chemistries, which is a powerful aspect of this project. The protein WDR91 (WD Repeat Domain 91) is of prime interest in the research for ASO trafficking modulators as it is an important factor that participates in the negative regulation of phosphatidylinositol–3–phosphate (PtdIns3P) allowing the early-to-late endosome conversion[53,54]. This protein represents a strong candidate as ASO activity enhancer and shows that ASOs productive release in cytosol could mainly occur during early endosome maturation or from the late endosomes as supported by other studies[55,56]. Furthermore, these data support other studies highlighting WDR proteins 81 and 91 as important mediators of release and efficacy of internalized reoviruses or antibody-drug conjugates in cells during the early endosome maturation or from the late endosomes[57,58].

In this study, we chose to focus on proteins that promote internalized ASOs activity but it would also be interesting to investigate in more details the protein inhibitors that were identified during the screen using the same experimental design. This work thus paves the way for future investigation which may reveal additional promising candidates.

Overall, our findings contribute to a better characterization and identification of protein modulators of ASO activity (activators or inhibitors) which is a valuable information for

potential new therapeutic avenue. Strong, *in vitro* validated ASO modulators could be inhibited or overexpressed in *in vivo* experiments to evaluate and confirm an increase of ASO potency. Acting on the level of such modulators or directly on ASO-modulators interaction could shift the balance towards a more productive ASO activity and thus, trigger an exacerbated inhibitory effect and a global increase in the corresponding ASO therapeutic index.

MATERIALS AND METHODS

Cell lines and lentiviral library

501Mel and U2OS cells were acquired from ATCC. Before experiments, all cells were regularly tested for absence of mycoplasma. Culture and sub-culturing were performed in RPMI-1640 (Gibco) for 501Mel and Mc Coy's 5A (Gibco) for A549, supplemented with 10% fetal bovine serum (FBS) (Gibco), 2mM L-glutamine (Gibco) and 1% penicillin/streptomycin, (Gibco) and cultured at 37°C in a humidified incubator with 5% CO_2. Transfections and infections were performed in the same media but without antibiotics and with a decomplemented serum (30 minutes at 56°C).

Antisense oligonucleotides

miRCURY LNA™ Target site blockers TSB-C1 (ACTTTATTACAATCAT) and TSB-T3 (ACACAGTGGCAAACAC) were designed and obtained from Qiagen and reconstituted in nuclease-free water (Invitrogen). tc-TSB-C1 and tc-TSB-T3 were synthesized from SQY Therapeutics (Montigny le Bretonneux) as fully modified tcDNA-PS ASOs. The TSB-C1 and tc-TSB-C1 controls have no significant match to any annotated human 3'UTR. ING2 LNA Gapmer (TACGTTGGCTTGTTCA) was designed and obtained from Qiagen and reconstituted in nuclease-free water (Invitrogen).

siRNAs

All siRNAs were purchased from Santa Cruz (Negative Control A sc-37007; WDR91 sc-89398; WBSCR16 sc-89899; FH sc-105377; ELMOD1 sc-77261; TADA2B sc-156169; ANXA2 sc-270151)

Generation of 501Mel knockout library

Transduction of 120 million mycoplasma negative 501Mel cells at 60% confluence was performed in T175 flasks (standard - Sarstedt) with the Brunello knockout pooled lentiviral library from Addgene (# 73179-LV) and in RPMI-1640 decomplemented medium (Gibco) without antibiotics. The Brunello pooled lentiviral library contains 76,441 single guides RNAs (sgRNAs), targeting 19,114 coding genes (4 sgRNAs per gene). A multiplicity of infection (MOI) of 0.4 was selected to ensure that every single cell is infected with only one sgRNA. 24h later, the infectious medium was replaced by a fresh complete medium. After 48h, infected cells were positively selected with 2.5ug/mL puromycin (InvivoGen) during 7 days. Following selection and expansion of the surviving cells, around 350 million cells were recovered. A dry pellet of 100 million cells was prepared for gDNA extraction and sequencing. The remaining cells were used for the subsequent reverse transfection.

RNA interference, ASO treatments and proliferation assay

501Mel naïve cells. Reverse-transfections of siRNAs were performed in 60mm dishes (standard - Sarstedt) with 224,000 cells per dish and for 48h in RPMI-1640 decomplemented medium without antibiotics. Briefly, 1mL lipoplexes layers were formed with Lipofectamine 2000 (Invitrogen) and the siRNA concentrations were set to 30nM in a final 3mL volume after addition of the cells on top of the lipoplexes. For all the transfections, lipoplexes were formed in OptiMEM®. After 16h incubation, the medium was replaced by a fresh complete medium without antibiotics. After 48h, the cells were recovered, counted with a Neubauer counting chamber and a second reverse-transfection was performed in 96-well plates (standard F-Sarstedt) with 3000 cells per well and with either the siRNA alone (at 30nM final concentration) or a combination of siRNA (30nM) and tc-TSB-T3 at a final concentration of 50nM in a final volume of 150uL (100uL of cells on top of 50uL of lipoplexes). After 16h incubation, the medium was replaced by a fresh 150uL complete medium without antibiotics. After 4 days following to the second transfection, the cell viability was measured with 0.5% crystal violet (10 minutes at RT, followed by three PBS washes, 100uL of 100% EtOH solubilization and absorbance reading at 590nm using a Tecan Infinite F200 Pro reader).
U2OS cells. Reverse-transfections of siRNAs were performed in 60mm dishes (standard - Sarstedt) with 220,000 cells per dish and for 48h in decomplemented Mc Coy's 5A medium without antibiotics. Cell density was optimized so these cells are efficiently transfected between 20 and 30% confluence. The procedure was the same as described above except that the siRNA reverse-transfection was performed with RNAiMax (Invitrogen) and the medium change was performed 6h later. After 48h, the medium was replaced by 2mL of a fresh decomplemented Mc Coy's 5A medium without antibiotics and a forward transfection with RNAiMax was performed in the same plate with the ING2 Gapmer (at 70nM final concentration) in a final volume of 3mL (1mL of lipoplexes on top of the cells). After 48h following to the second transfection, total RNA was extracted for further RT-qPCR analysis.
501Mel knockout library. Reverse-transfections of tc-TSB-T3 and C1 were performed in 150mm dishes (standard - Sarstedt) with 1.5 million knockout cells per dish and for 72h in RPMI-1640 decomplemented medium without antibiotics. Briefly, 10mL lipoplexes layers were formed with Lipofectamine 2000 (Invitrogen) and the respective ASOs concentrations were set to 50nM in a final 24mL volume after addition of the cells on top of the lipoplexes. For the transfections, lipoplexes were formed in OptiMEM® and the mycoplasma-negative knockout cells have been sub-cultured 24h before in T175 flasks (standard - Sarstedt). The cells confluency at the day of transfection was always between 50 and 80%. After 7h of transfection, the medium was replaced by a fresh complete medium without antibiotics. To ensure a coverage of 400 cells per guide RNA in our library, a total of 32 million cells was transfected with either the tc-TSB-T3 or C1. Thus, 22 dishes were used per oligonucleotide transfection. After 72h of transfection, surviving cells were recovered and pellets of 100 million cells were kept at -80°C until further processing.

NGS sequencing library preparation

Frozen pellets of 100 million transfected surviving cells (and from non-treated knockout library) in 50mL poplypropylene tubes (Sarstedt) were thawed on ice for 20 minutes and lysed at room temperature. Genomic DNA was purified according to the manufacturer's instructions (NucleoBond HMW DNA, Macherey-Nagel). A total of 280ug of genomic DNAs was used for PCR amplification of sgRNA sequences, using the Herculase II Fusion polymerase (Agilent). Illumina P5- and P7-barcoded adaptors were used and PCR amplification and quality controls have been carried out as described by Zhang laboratory (Joung *et al*, 2017). Amplified PCR products were purified using AMPure XP beads (Beckman Coulter) according to the manufacturer's instructions, eluted in 14uL of nuclease-free water (Invitrogen) and stored at -

20°C until Bioanalyzer quality control (TapeStation 4200, Agilent) was used to measure the size, quality and concentration. The pooled samples were sequenced using Illumina NGS sequencing platform (Novaseq6000 – Institut Curie CRISPR'it Platform).

NGS data analysis

MAGeCK was used to extract sgRNA read counts from the samples fastq.gz files (mageck count program with the --norm-method median option). For each sgRNA, we transformed the read counts onto M (log ratio) and A (mean average): M = log2(sgRNA_count_in_TRT+1) - log2(sgRNA_count_in_CTL+1), and A = mean (count_TRT, count_CTL) in log2 scale. Fold-changes between TRT and CTL conditions were also computed from the M values of each sgRNA.

RNA extraction and RT-qPCR analysis

Total RNA form cell lysates was obtained using a NucleoSpin® RNA kit (Macherey-Nagel), according to the manufacturer's instructions and with on-column DNAse treatment. After Nanodrop evaluation of purity and concentration, 500ng of RNA was used for reverse-transcription (MultiScribe RT – Applied Biosystems). Obtained cDNA was diluted to 2.5ng/uL and used as template for qPCR using a QuantStudio5 system (Applied Biosystems). SYBR Green (PowerSYBR® Green PCR Master Mix – Applied Biosystems) was used according to the manufacturer's instructions. For each sample measurement, 3 technical replicates were performed. TBP was used as internal standard. TYRP1 and ING2 primers were purchased from and the sequences are shown in the table 1 below.

Protein isolation and Western blotting

Total protein extracts were obtained by resuspension of PBS-washed cell pellets in 40uL of ice-cold RIPA buffer (Tris-HCl 50 mM, ph7.4, NaCl 150 mM, Sodium Deoxycholate 0.5%, Triton 1%, SDS 0.1%), including protease inhibitor cocktail (Sigma-Aldrich, P8340) and centrifugation at 16,000xg for 15min at 4°C. Proteins quantification from the cleared lysates was performed using a Pierce™ BCA Assay kit (Thermo scientific). After 4-12% SDS-PAGE in NuPAGE MES buffer (Invitrogen), proteins were transferred onto PVDF membranes with a turbo transfer system (BIO-RAD) for 10 minutes at 25V and 2.5A. After transfer, the membranes were washed in Tris-buffered saline and 0.1% Tween 20 (TBST) and blocked for 30 minutes at room temperature in a solution of TBST + 5% w/v non-fat dry milk. Blocked membranes were washed three times in TBST for 5 minutes and diluted primary antibody was incubated at 4°C overnight with shaking. The diluted HRP-conjugated secondary antibody was added for 1h at room temperature with shaking, after three TBST washes of 5 minutes. Imaging was performed after ECL reagent addition and chemiluminescence detection with G:Box Chemi XX6 imager from Syngene. RAB17 antibody was purchased from Cell Signaling Technology (#8013). ANXA2 antibody was purchased from Santa Cruz (sc-28385).

Statistical analysis

Data are presented as mean of at least three independent biological replicates ± SD. P-values were calculated by two-sided unpaired *t*-tests with Welch's correction.

ACKNOWLEDGMENTS

The authors thank the SFR Biosit L3 platform of Rennes University for providing the required facility for performing the lentiviral infections. The authors also thank the Institut Curie (Genetic screen platform CRISPR'it) for performing the NGS sequencing and SQY Therapeutics for providing the tricyclo-ASO molecules. This study received financial support from the Agence Nationale de la Recherche (ANR).

AUTHOR CONTRIBUTIONS

G.M. and R.P. conceived and analyzed the experiments. G.M. performed the experiments. M.A. analyzed the NGS raw data. A.M. helped in the library preparation. A.Go. and A.Ga. helped in analyzing and interpreting the data. A.B. performed the NGS sequencing. G.M. wrote the manuscript. All the authors reviewed the manuscript.

DISCLOSURE AND COMPETING INTERESTS STATEMENT
The authors declare no competing financial interests.

REFERENCES

[1] Stanley T. Crooke et al., "Antisense Technology: A Review," *The Journal of Biological Chemistry* 296 (February 16, 2021): 100416, https://doi.org/10.1016/j.jbc.2021.100416.

[2] J. Kim et al., "Patient-Customized Oligonucleotide Therapy for a Rare Genetic Disease," *The New England Journal of Medicine* 381, no. 17 (October 24, 2019): 1644–52, https://doi.org/10.1056/NEJMoa1813279.

[3] Stanley T Crooke et al., "Cellular Uptake and Trafficking of Antisense Oligonucleotides," *Nature Biotechnology* 35, no. 3 (March 1, 2017): 230–37, https://doi.org/10.1038/nbt.3779.

[4] Xin Xie et al., "Recent Advances in Targeting the 'Undruggable' Proteins: From Drug Discovery to Clinical Trials," *Signal Transduction and Targeted Therapy* 8, no. 1 (September 6, 2023): 1–71, https://doi.org/10.1038/s41392-023-01589-z.

[5] Martin Egli and Muthiah Manoharan, "Chemistry, Structure and Function of Approved Oligonucleotide Therapeutics," *Nucleic Acids Research* 51, no. 6 (March 7, 2023): 2529–73, https://doi.org/10.1093/nar/gkad067.

[6] Tina Nie, "Eplontersen: First Approval," *Drugs*, February 28, 2024, https://doi.org/10.1007/s40265-024-02008-5.

[7] Haoyu Xiong, Rakesh N. Veedu, and Sarah D. Diermeier, "Recent Advances in Oligonucleotide Therapeutics in Oncology," *International Journal of Molecular Sciences* 22, no. 7 (March 24, 2021): 3295, https://doi.org/10.3390/ijms22073295.

[8] Maria Gagliardi and Ana Tari Ashizawa, "The Challenges and Strategies of Antisense Oligonucleotide Drug Delivery," *Biomedicines* 9, no. 4 (April 16, 2021): 433, https://doi.org/10.3390/biomedicines9040433.

[9] Suzan M Hammond et al., "Delivery of Oligonucleotide-based Therapeutics: Challenges and Opportunities," *EMBO Molecular Medicine* 13, no. 4 (April 9, 2021): e13243, https://doi.org/10.15252/emmm.202013243.

[10] R.L. Juliano et al., "Cellular Uptake and Intracellular Trafficking of Oligonucleotides: Implications for Oligonucleotide Pharmacology," *Nucleic Acid Therapeutics* 24, no. 2 (April 1, 2014): 101–13, https://doi.org/10.1089/nat.2013.0463.

[11] Alexander Klipp, Michael Burger, and Jean-Christophe Leroux, "Get out or Die Trying: Peptide- and Protein-Based Endosomal Escape of RNA Therapeutics," *Advanced Drug Delivery Reviews* 200 (September 1, 2023): 115047, https://doi.org/10.1016/j.addr.2023.115047.

[12] Steven F. Dowdy et al., "Delivery of RNA Therapeutics: The Great Endosomal Escape!," *Nucleic Acid Therapeutics* 32, no. 5 (October 1, 2022): 361–68, https://doi.org/10.1089/nat.2022.0004.

[13] Philippine Aupy et al., "The Use of Tricyclo-DNA Oligomers for the Treatment of Genetic Disorders," *Biomedicines* 6, no. 1 (December 22, 2017): 2, https://doi.org/10.3390/biomedicines6010002.

[14] "Delivery Is Key: Lessons Learnt from Developing Splice-switching Antisense Therapies | EMBO Molecular Medicine," accessed March 27, 2024, https://www.embopress.org/doi/full/10.15252/emmm.201607199.

[15] Feryal Alhamadani et al., "Adverse Drug Reactions and Toxicity of the Food and Drug Administration-Approved Antisense Oligonucleotide Drugs," *Drug Metabolism and Disposition: The Biological Fate of Chemicals* 50, no. 6 (June 2022): 879–87, https://doi.org/10.1124/dmd.121.000418.

[16] Xue-hai Liang et al., "Identification and Characterization of Intracellular Proteins That Bind Oligonucleotides with Phosphorothioate Linkages," *Nucleic Acids Research* 43, no. 5 (March 11, 2015): 2927–45, https://doi.org/10.1093/nar/gkv143.

[17] Stanley T. Crooke et al., "The Interaction of Phosphorothioate-Containing RNA Targeted Drugs with Proteins Is a Critical Determinant of the Therapeutic Effects of These Agents," *Journal of the American Chemical Society* 142, no. 35 (September 2, 2020): 14754–71, https://doi.org/10.1021/jacs.0c04928.

[18] Xue-Hai Liang et al., "Hsp90 Protein Interacts with Phosphorothioate Oligonucleotides Containing Hydrophobic 2′-Modifications and Enhances Antisense Activity," *Nucleic Acids Research* 44, no. 8 (May 5, 2016): 3892–3907, https://doi.org/10.1093/nar/gkw144.

[19] Crooke et al., "Cellular Uptake and Trafficking of Antisense Oligonucleotides."

[20] Colton M. Miller et al., "Stabilin-1 and Stabilin-2 Are Specific Receptors for the Cellular Internalization of Phosphorothioate-Modified Antisense Oligonucleotides (ASOs) in the Liver," *Nucleic Acids Research* 44, no. 6 (April 7, 2016): 2782–94, https://doi.org/10.1093/nar/gkw112.

[21] Thijs Van de Vyver, Stefaan C. De Smedt, and Koen Raemdonck, "Modulating Intracellular Pathways to Improve Non-Viral Delivery of RNA Therapeutics," *Advanced Drug Delivery Reviews* 181 (February 1, 2022): 114041, https://doi.org/10.1016/j.addr.2021.114041.

[22] Brendan T Finicle et al., "Simultaneous Inhibition of Endocytic Recycling and Lysosomal Fusion Sensitizes Cells and Tissues to Oligonucleotide Therapeutics," *Nucleic Acids Research* 51, no. 4 (February 28, 2023): 1583–99, https://doi.org/10.1093/nar/gkad023.

[23] Alexander N. Kapustin et al., "Antisense Oligonucleotide Activity in Tumour Cells Is Influenced by Intracellular LBPA Distribution and Extracellular Vesicle Recycling," *Communications Biology* 4 (November 1, 2021): 1241, https://doi.org/10.1038/s42003-021-02772-0.

[24] Timothy R. Wagenaar et al., "Identification of the Endosomal Sorting Complex Required for Transport-I (ESCRT-I) as an Important Modulator of Anti-MiR Uptake by Cancer Cells," *Nucleic Acids Research* 43, no. 2 (January 30, 2015): 1204–15, https://doi.org/10.1093/nar/gku1367.

[25] Shiyu Wang et al., "Membrane Destabilization Induced by Lipid Species Increases Activity of Phosphorothioate-Antisense Oligonucleotides," *Molecular Therapy - Nucleic Acids* 13 (December 2018): 686–98, https://doi.org/10.1016/j.omtn.2018.10.011.

[26] Peter Lorenz et al., "Nucleocytoplasmic Shuttling: A Novel in Vivo Property of Antisense Phosphorothioate Oligodeoxynucleotides," *Nucleic Acids Research* 28, no. 2 (January 15, 2000): 582–92.

[27] "A Stress-Induced Response Complex (SIRC) Shuttles MiRNAs, SiRNAs, and Oligonucleotides to the Nucleus," accessed March 27, 2024, https://www.pnas.org/doi/epdf/10.1073/pnas.1721346115.

[28] Crooke et al., "The Interaction of Phosphorothioate-Containing RNA Targeted Drugs with Proteins Is a Critical Determinant of the Therapeutic Effects of These Agents."

[29] Liang et al., "Identification and Characterization of Intracellular Proteins That Bind Oligonucleotides with Phosphorothioate Linkages."

[30] Alfred Hanswillemenke et al., "Profiling the Interactome of Oligonucleotide Drugs by Proximity Biotinylation," *Nature Chemical Biology*, January 17, 2024, https://doi.org/10.1038/s41589-023-01530-z.

[31] Christoph Bock et al., "High-Content CRISPR Screening," *Nature Reviews Methods Primers* 2, no. 1 (February 10, 2022): 1–23, https://doi.org/10.1038/s43586-021-00093-4.

[32] Olivier Petitjean et al., "Genome-Wide CRISPR-Cas9 Screen Reveals the Importance of the Heparan Sulfate Pathway and the Conserved Oligomeric Golgi Complex for Synthetic Double-Stranded RNA Uptake and Sindbis Virus Infection," *MSphere* 5, no. 6 (November 11, 2020): e00914-20, https://doi.org/10.1128/mSphere.00914-20.

[33] C. Kimberly Tsui et al., "CRISPR-Cas9 Screens Identify Regulators of Antibody–Drug Conjugate Toxicity," *Nature Chemical Biology* 15, no. 10 (October 2019): 949–58, https://doi.org/10.1038/s41589-019-0342-2.

[34] Douglas Ross-Thriepland et al., "Arrayed CRISPR Screening Identifies Novel Targets That Enhance the Productive Delivery of MRNA by MC3-Based Lipid Nanoparticles," *SLAS Discovery* 25, no. 6 (July 2020): 605–17, https://doi.org/10.1177/2472555220925770.

[35] Moira A. McMahon et al., "GOLGA8 Increases Bulk Antisense Oligonucleotide Uptake and Activity in Mammalian Cells," *Molecular Therapy. Nucleic Acids* 32 (March 27, 2023): 289–301, https://doi.org/10.1016/j.omtn.2023.03.017.

[36] David Gilot et al., "A Non-Coding Function of TYRP1 MRNA Promotes Melanoma Growth," *Nature Cell Biology* 19, no. 11 (November 2017): 1348–57, https://doi.org/10.1038/ncb3623.

[37] Philippine Aupy et al., "Identifying and Avoiding TcDNA-ASO Sequence-Specific Toxicity for the Development of DMD Exon 51 Skipping Therapy," *Molecular Therapy. Nucleic Acids* 19 (November 27, 2019): 371–83, https://doi.org/10.1016/j.omtn.2019.11.020.

[38] "Lowering Mutant Huntingtin Using Tricyclo-DNA Antisense Oligonucleotides As a Therapeutic Approach for Huntington's Disease - PubMed," accessed March 27, 2024, https://pubmed.ncbi.nlm.nih.gov/31184975/.

[39] "Annexin A2 Facilitates Endocytic Trafficking of Antisense Oligonucleotides - PubMed."

[40] Gilot et al., "A Non-Coding Function of TYRP1 MRNA Promotes Melanoma Growth."

[41] Emily Linnane et al., "Differential Uptake, Kinetics and Mechanisms of Intracellular Trafficking of next-Generation Antisense Oligonucleotides across Human Cancer Cell Lines," *Nucleic Acids Research* 47, no. 9 (May 21, 2019): 4375–92, https://doi.org/10.1093/nar/gkz214.

[42] "ING2 Tumor Suppressive Protein Translocates into Mitochondria and Is Involved in Cellular Metabolism Homeostasis | Oncogene," accessed March 27, 2024, https://www.nature.com/articles/s41388-021-01832-3.

[43] Gilot et al., "A Non-Coding Function of TYRP1 MRNA Promotes Melanoma Growth."

[44] "WBSCR16 Is a Guanine Nucleotide Exchange Factor (GEF) Important for Mitochondrial Fusion - PMC," accessed March 27, 2024, https://www.ncbi.nlm.nih.gov/pmc/articles/PMC5562410/.

[45] Kiran Todkar, Lilia Chikhi, and Marc Germain, "Mitochondrial Interaction with the Endosomal Compartment in Endocytosis and Mitochondrial Transfer," *Mitochondrion* 49 (November 2019): 284–88, https://doi.org/10.1016/j.mito.2019.05.003.

[46] Anupam Das et al., "Endosome–Mitochondria Interactions Are Modulated by Iron Release from Transferrin," *The Journal of Cell Biology* 214, no. 7 (September 9, 2016): 831, https://doi.org/10.1083/jcb.201602069.

[47] Karen Cuellar et al., "Biosynthesis of Chondroitin and Heparan Sulfate in Chinese Hamster Ovary Cells Depends on Xylosyltransferase II*," *Journal of Biological Chemistry* 282, no. 8 (February 23, 2007): 5195–5200, https://doi.org/10.1074/jbc.M611048200.

[48] Jessica B. Blackburn, Zinia D'Souza, and Vladimir V. Lupashin, "Maintaining Order: COG Complex Controls Golgi Trafficking, Processing, and Sorting," *Febs Letters* 593, no. 17 (September 2019): 2466–87, https://doi.org/10.1002/1873-3468.13570.

[49] Petitjean et al., "Genome-Wide CRISPR-Cas9 Screen Reveals the Importance of the Heparan Sulfate Pathway and the Conserved Oligomeric Golgi Complex for Synthetic Double-Stranded RNA Uptake and Sindbis Virus Infection."

[50] Xue-Hai Liang et al., "Golgi-Endosome Transport Mediated by M6PR Facilitates Release of Antisense Oligonucleotides from Endosomes," *Nucleic Acids Research* 48, no. 3 (February 20, 2020): 1372–91, https://doi.org/10.1093/nar/gkz1171.

[51] Tamás Letoha et al., "Contribution of Syndecans to Lipoplex-Mediated Gene Delivery," *European Journal of Pharmaceutical Sciences* 49, no. 4 (July 16, 2013): 550–55, https://doi.org/10.1016/j.ejps.2013.05.022.

[52] Abdelatif Elouahabi and Jean-Marie Ruysschaert, "Formation and Intracellular Trafficking of Lipoplexes and Polyplexes," *Molecular Therapy* 11, no. 3 (March 1, 2005): 336–47, https://doi.org/10.1016/j.ymthe.2004.12.006.

[53] Kai Liu et al., "WDR91 Is a Rab7 Effector Required for Neuronal Development," *Journal of Cell Biology* 216, no. 10 (October 2, 2017): 3307–21, https://doi.org/10.1083/jcb.201705151.

[54] Nan Liu, Kai Liu, and Chonglin Yang, "WDR91 Specifies the Endosomal Retrieval Subdomain for Retromer-Dependent Recycling," *The Journal of Cell Biology* 221, no. 12 (December 12, 2022), https://doi.org/10.1083/jcb.202203013.

[55] Colton M. Miller et al., "Endosomal Escape of Antisense Oligonucleotides Internalized by Stabilin Receptors Is Regulated by Rab5C and EEA1 During Endosomal Maturation," *Nucleic Acid Therapeutics* 28, no. 2 (April 1, 2018): 86–96, https://doi.org/10.1089/nat.2017.0694.

[56] "Annexin A2 Facilitates Endocytic Trafficking of Antisense Oligonucleotides - PubMed," accessed March 27, 2024, https://pubmed.ncbi.nlm.nih.gov/27378781/.

[57] Anthony J. Snyder, Andrew T. Abad, and Pranav Danthi, "A CRISPR-Cas9 Screen Reveals a Role for WD Repeat-Containing Protein 81 (WDR81) in the Entry of Late Penetrating Viruses," *PLoS Pathogens* 18, no. 3 (March 2022): e1010398, https://doi.org/10.1371/journal.ppat.1010398.

[58] Tsui et al., "CRISPR-Cas9 Screens Identify Regulators of Antibody–Drug Conjugate Toxicity."